International Journal of Innovative
Computing, Information and Control
Volume **9**, Number **12**, December **2013**

 ISSN 1349-4198
pp. 4793–4809

CHATTERING-FREE SMC WITH UNIDIRECTIONAL AUXILIARY SURFACES FOR NONLINEAR SYSTEM WITH STATE CONSTRAINTS

Jian Fu, Qing-Xian Wu and Ze-Hui Mao

Department of Automation
Nanjing University of Aeronautics and Astronautics
No. 29, Yudao Street, Baixia District, Nanjing 210016, P. R. China
fujian1986216@126.com; { wuqingxian; zehuimao }@nuaa.edu.cn

Received December 2012; revised April 2013

Abstract. *This paper presents a chattering-free sliding mode control with unidirectional auxiliary surfaces (UAS-SMC) for nonlinear system with state constraints. In contrast to existing chattering-free sliding mode control (SMC) methods, the proposed strategy shows another way to eliminate the chattering phenomenon. Moreover, the positively invariant set in UAS-SMC is used to constrain the system states. Stability analysis is provided based on Lyapunov stability theory. Finally, a numerical example is given to show the benefits and properties of the proposed algorithm.*
Keywords: UAS-SMC, Sliding mode, Nonlinear system, Chattering-free, Simplified approaching law, State constraints

1. **Introduction.** The sliding mode control (SMC) strategy has attracted considerable attention in the last decades. Due to its high robust features and convenience for real implementation, this scheme has been widely applied in many applications such as time-delay system, reusable launch vehicle, fuzzy system and disturbance observer [1-5]. However, the existence of state constraints is an important problem which we should take into account. If we ignore this problem, the performance of controller may degrade, or in worst cases, the system becomes unstable [6-8].

Thus, set invariance theory is introduced to solve this problem. The foundation of this theory is a positively-invariant (PI) set Q_i resulting in trajectories remaining in Q_i for all subsequent times. According to the selected shapes, PI sets could be divided into three different kinds: polyhedrons offer good accuracy in expense of complexity, while ellipsoids are, in that sense, the opposite [9]. Semi-ellipsoidal sets offer a convenient tradeoff. In this approach, an invariant ellipsoid, which may exceed the constraints, is sought under the condition that its intersection with the constraints retains the PI property [10].

The vast majority of research dealing with PI set is related to linear systems. And only a few papers have addressed the issue of state constraints with sliding mode control (SMC) [11]. In this paper, we proposed a design method called sliding mode control with unidirectional auxiliary surfaces (UAS-SMC) for nonlinear system with state constraints. Unidirectional auxiliary surfaces, which naturally form PI sets, are introduced in this method. The main advantage of this design is that system states are constrained by unidirectional auxiliary surfaces instead of switching surfaces. Then, constraints are guaranteed when system states leaving the switching surfaces. A chattering-free approaching law is given to eliminate the chattering phenomenon in the controller. And this paper is organized as follows. Preliminary is given in Section 2. Section 3 introduces the control

design of chattering-free UAS-SMC controller, while main results are presented in Section 4. Section 5 contains simulation results, and Section 6 concludes this paper.

2. **Preliminary.** Consider the following nonlinear system:

$$\dot{\boldsymbol{x}} = \boldsymbol{f}(\boldsymbol{x}) + \boldsymbol{g}(\boldsymbol{x})\boldsymbol{u} \tag{1}$$

where $\boldsymbol{x} = [x_1, \cdots, x_n]^T \in R^n$ is the system state vector, $u \in R^n$ is control input, $\boldsymbol{f}(\boldsymbol{x}) \in R^n$, $\boldsymbol{g}(\boldsymbol{x}) \in R^{n\times n}$ are continuous functions. It is assumed that $\boldsymbol{g}(\boldsymbol{x})$ is invertible for all $\boldsymbol{x}$. State constraints are usually formulated as a set of linear inequalities:

$$\psi_i = \{(x_i, \int x_i) \,|n_i \le x_i \le m_i\}, \quad i = 1, \cdots, n \tag{2}$$

where term $\int x_i \, dt$ is denoted as $\int x_i$. The purpose of this paper is to design a chattering-free UAS-SMC controller under state constraints $\psi = [\psi_1, \cdots, \psi_n]^T$.

3. **Control Design.** In this section, we present the design process of UAS-SMC controller. The whole process is divided into four steps:

Step 1: The switching surfaces for the state $\boldsymbol{x}$ in system (1) are given by:

$$\begin{aligned} \boldsymbol{s}_1 &= \boldsymbol{x} + \boldsymbol{\xi}_1 \int \boldsymbol{x} = 0 \\ \boldsymbol{s}_2 &= \boldsymbol{x} + \boldsymbol{\xi}_2 \int \boldsymbol{x} = 0 \end{aligned} \tag{3}$$

where $\boldsymbol{s}_1 = [s_{11}, \ldots, s_{1n}]^T$, $\boldsymbol{s}_2 = [s_{21}, \ldots, s_{2n}]^T$, $\int \boldsymbol{x} = [\int x_1, \ldots, \int x_n]^T$, $\boldsymbol{\xi}_1 = \text{diag}\{\xi_{11}, \ldots, \xi_{1n}\}$, $\boldsymbol{\xi}_2 = \text{diag}\{\xi_{21}, \ldots, \xi_{2n}\}$, $\xi_{1i} > \xi_{2i} > 0$, $i = 1, \ldots, n$. $\xi_{1i} > 0$, $\xi_{2i} > 0$ is given to guarantee the stability of switching surfaces $s_{1i} = 0$, $s_{2i} = 0$. And $\xi_{1i} > \xi_{2i}$ is used to avoid the overlap of switching surfaces $s_{1i} = 0$, $s_{2i} = 0$.

Step 2: Based on the switching surfaces s_{1i}, s_{2i}, the No. $0_i, \ldots, 3_i$ subspaces can be defined in Figure 1, where

$$\begin{aligned} &\text{No. } 0_i \text{ subspace} = \{(x_i, \int x_i) | s_{1i} < 0, s_{2i} < 0\}; \\ &\text{No. } 1_i \text{ subspace} = \{(x_i, \int x_i) | s_{1i} < 0, s_{2i} \ge 0\}; \\ &\text{No. } 2_i \text{ subspace} = \{(x_i, \int x_i) | s_{1i} \ge 0, s_{2i} < 0\}; \\ &\text{No. } 3_i \text{ subspace} = \{(x_i, \int x_i) | s_{1i} \ge 0, s_{2i} \ge 0\} \end{aligned} \tag{4}$$

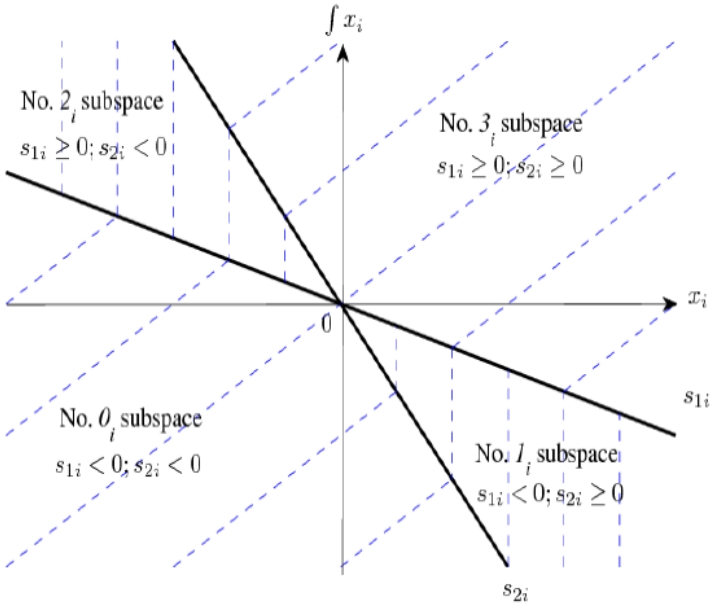

FIGURE 1. The four subspaces

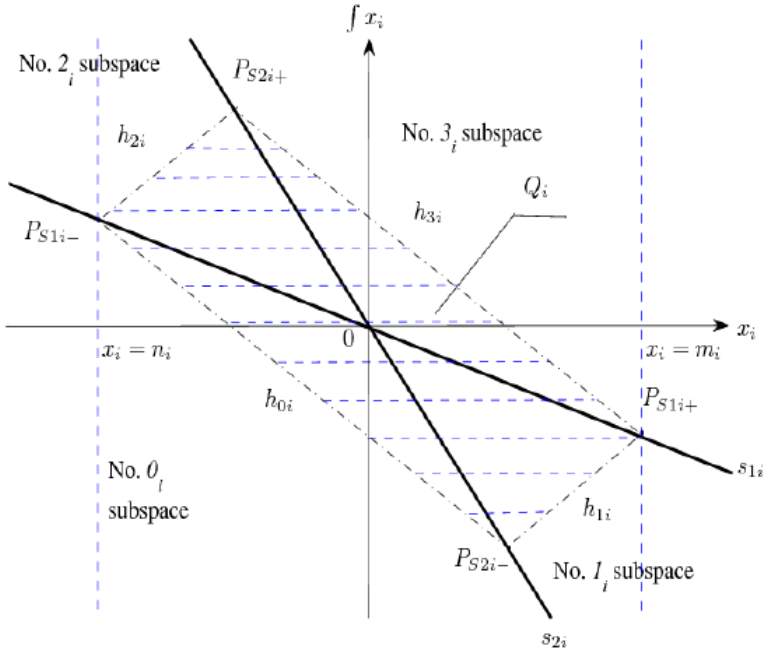

FIGURE 2. The UAS h_{0i}, h_{1i}, h_{2i}, h_{3i}

The appropriate points P_{s1i+}, P_{s1i-}, P_{s2i+} and P_{s2i-} on switching surface s_{1i}, s_{2i} should be selected inside the state constraint $n_i \le x_i \le m_i$, where points P_{s1i+}, P_{s2i-} are located in the fourth quadrant, and points P_{s1i-}, P_{s2i-} are located in the second quadrant, as shown in Figure 2. It is noted that:

$$\begin{aligned} s_{1i}(P_{s1i+}) = 0; \quad s_{1i}(P_{s1i-}) = 0 \\ s_{2i}(P_{s2i+}) = 0; \quad s_{2i}(P_{s2i-}) = 0 \end{aligned} \tag{5}$$

The lines $P_{s1i-}P_{s2i-}$, $P_{s1i+}P_{s2i-}$, $P_{s1i-}P_{s2i+}$, $P_{s1i+}P_{s2i+}$ defined in Figure 2 are unidirectional auxiliary surfaces (UAS) h_{0i}, h_{1i}, h_{2i}, h_{3i}. The formulae of these UAS are given as follows:

$$h_{ki} = \omega_{ki1} x_i + \omega_{ki2} \int x_i + M_i \tag{6}$$

where $k \in \{0, 1, 2, 3\}$, $\omega_{ki1} \neq 0$, $M_i > 0$. The coefficients ω_{1i1}, ω_{2i1} in Equation (6) should satisfy $\omega_{1i1} < 0$, $\omega_{2i1} > 0$, which is a sufficient condition for the existence of chattering-free UAS-SMC controller [12]. The coefficients ω_{ki1}, ω_{ki2} should satisfy the simplified condition (7) in this paper.

$$\omega_{0i1} = -\omega_{3i1}, \quad \omega_{0i2} = -\omega_{3i2}, \quad \omega_{1i1} = -\omega_{2i1}, \quad \omega_{1i2} = -\omega_{2i2} \tag{7}$$

Step 3: The UAS in Figure 2 would be utilized to design control input $\boldsymbol{u}$ when the states are moving in No. $0_i, \ldots, 3_i$ subspaces. The current UAS for state x_i is given as:

$$h_i = \omega_{i1} x_i + \omega_{i2} \int x_i + M_i, \quad i = 1, \ldots, n \tag{8}$$

where $M_i > 0$ is a constant value,

$$\omega_{i1} = \begin{cases} \omega_{0i1} & s_{1i} < 0, s_{2i} < 0 \\ \omega_{1i1} & s_{1i} < 0, s_{2i} \ge 0 \\ \omega_{2i1} & s_{1i} \ge 0, s_{2i} < 0 \\ \omega_{3i1} & s_{1i} \ge 0, s_{2i} \ge 0 \end{cases}, \quad \omega_{i2} = \begin{cases} \omega_{0i2} & s_{1i} < 0, s_{2i} < 0 \\ \omega_{1i2} & s_{1i} < 0, s_{2i} \ge 0 \\ \omega_{2i2} & s_{1i} \ge 0, s_{2i} < 0 \\ \omega_{3i2} & s_{1i} \ge 0, s_{2i} \ge 0 \end{cases}$$

Consequently, the compact form of current UAS could be rewritten as:

$$\boldsymbol{h} = \boldsymbol{\Omega}_1 \boldsymbol{x} + \boldsymbol{\Omega}_2 \int \boldsymbol{x} + \boldsymbol{M} \tag{9}$$

where $\boldsymbol{h} = [h_1, \ldots, h_n]^T$, $\boldsymbol{\Omega}_1 = \text{diag}\{\omega_{11}, \ldots, \omega_{n1}\}$, $\boldsymbol{\Omega}_2 = \text{diag}\{\omega_{12}, \ldots, \omega_{n2}\}$, $\boldsymbol{M} = [M_1, \ldots, M_n]^T$.

Step 4: The UAS-SMC control input $\boldsymbol{u}$ for the nonlinear system (1) is designed by solving the equation

$$\dot{\boldsymbol{h}} = \boldsymbol{\Omega}_1(\boldsymbol{f}(\boldsymbol{x}) + \boldsymbol{g}(\boldsymbol{x})\boldsymbol{u}) + \boldsymbol{\Omega}_2 \cdot \boldsymbol{x} = \boldsymbol{N}$$

It follows that, the UAS-SMC control for system (1) can be expressed as:

$$\boldsymbol{u} = \boldsymbol{g}(\boldsymbol{x})^{-1}(-\boldsymbol{f}(\boldsymbol{x}) - \boldsymbol{\Omega}_1^{-1}\boldsymbol{\Omega}_2 \cdot \boldsymbol{x} + \boldsymbol{\Omega}_1^{-1} \cdot \boldsymbol{N}) \tag{10}$$

where coefficients $\boldsymbol{\Omega}_1$, $\boldsymbol{\Omega}_2\cdot$ can be found in Equation (9); $\boldsymbol{N} = [N_1, , \ldots, N_n]^T$, $N_i > 0$, $i = 1, \ldots, n$ are the approaching laws.

4. Main Results.

In this section, research for UAS-SMC theory falls into three different parts. The first part relates to the proof of stability in UAS-SMC theory. A discussion for positively invariant (PI) property of set Q_i is shown in the second part. In order to eliminate chattering phenomenon in UAS-SMC controller, a chattering-free approaching law is described in the last part.

4.1. Stability proof.

SMC is a widely studied technique which uses predefined switching surfaces $\boldsymbol{s}$ to guarantee the stability. So Lyapunov function for SMC is usually formulated as $V = 1/2 \cdot \boldsymbol{s}^T\boldsymbol{s}$. However, for the UAS-SMC theory, Lyapunov function is selected as a complex form

$$V = 1/2(\boldsymbol{M} - \boldsymbol{h})^T(\boldsymbol{M} - \boldsymbol{h}) \tag{11}$$

The proof for this Lyapunov function is given as follows.

Lemma 4.1. *For state x_i in system (1), the current UAS $h_i(x_i)$*

$$h_i(x_i) = \omega_{i1}x_i + \omega_{i2}\textstyle\int x_i + M_i, \quad i = 1, \ldots, n \tag{12}$$

is a continuous function.

Proof: The proof to Lemma 4.1 is done by the definition of current UAS. It is shown that current UAS $h_i(x_i)$ is switching between different subspaces from the definition in Equation (8). Without loss of generality, we assume that $h_i(x_i)$ is switching between No. 1_i and 3_i subspaces, where switching point $P(t)$ is given in Figure 3. The coordinate of P_{s1i+} is defined as (x, y). Note that point $P(t)$ located on line $0P_{s1i+}$ is found in the same quadrant of point P_{s1i+}. There exists $P(t) = (\lambda \cdot x, \lambda \cdot y)$, where $\lambda > 0$.

Definition of current UAS $h_i(x_i)$ also shows the relationship between $h_i(x_i)$ and $h_{ki}(x_i)$:

$$\begin{aligned} h_i(x_i) &= h_{1i}(x_i) = \omega_{1i1}x_i + \omega_{1i2}\textstyle\int x_i + M_i, \text{ when state } x_i \text{ in No. } 1_i \text{ subspace} \\ h_i(x_i) &= h_{3i}(x_i) = \omega_{3i1}x_i + \omega_{3i2}\textstyle\int x_i + M_i, \text{ when state } x_i \text{ in No. } 3_i \text{ subspace} \end{aligned} \tag{13}$$

It is shown in Figure 3 that point P_{s1i+} is located on UAS $h_{1i}(x_i)$ and $h_{3i}(x_i)$. The following conclusion is obtained:

$$\begin{aligned} h_{1i}(P_{s1i+}) &= \omega_{1i1} \cdot x + \omega_{1i2} \cdot y + M_i = 0 \\ h_{3i}(P_{s1i+}) &= \omega_{3i1} \cdot x + \omega_{3i2} \cdot y + M_i = 0 \end{aligned} \tag{14}$$

As we discussed before, the coordinate of $P(t)$ is defined as $(\lambda \cdot x, \lambda \cdot y)$, where $\lambda >0$. It follows that

$$\begin{aligned} h_{1i}(P(t)) &= \lambda \cdot (\omega_{1i1} \cdot x + \omega_{1i2} \cdot y + M_i) - \lambda \cdot M_i + M_i \\ h_{3i}(P(t)) &= \lambda \cdot (\omega_{3i1} \cdot x + \omega_{3i2} \cdot y + M_i) - \lambda \cdot M_i + M_i \end{aligned} \tag{15}$$

Considering Equation (14) and Equation (15), we have a conclusion that $h_{1i}(P(t)) = h_{3i}(P(t))$. Consequently, current UAS $h_i(x_i)$ is continuous while switching between No.

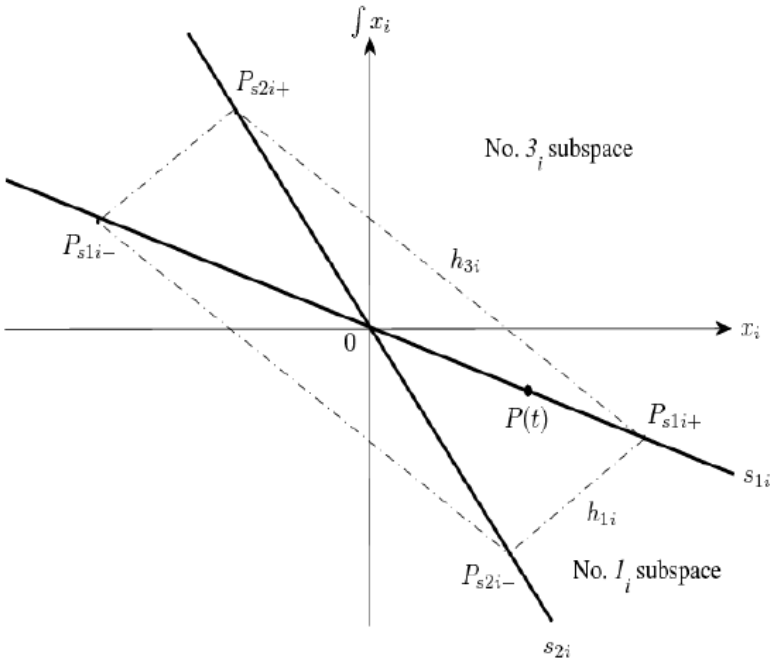

FIGURE 3. Switching point $P(t)$ between No. 1_i and 3_i subspaces

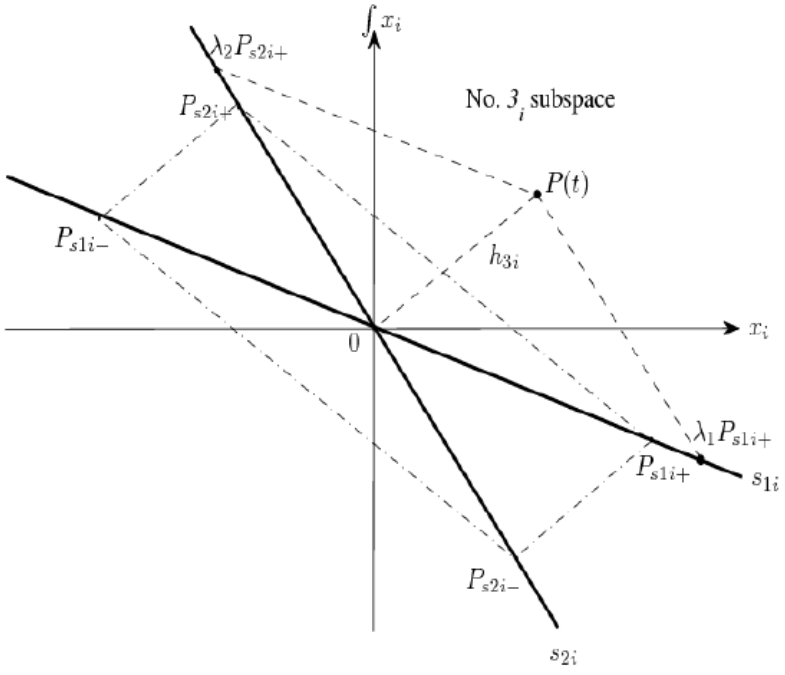

FIGURE 4. $P(t)$ in No. 3_i subspaces

1_i and 3_i subspaces. For the other subspaces, we have the same conclusion. So the current UAS $h_i(x_i)$ is a continuous function for state x_i in system (1).

Lemma 4.2. *For state x_i in system (1), current UAS $h_i(x_i)$*

$$h_i(x_i) = \omega_{i1} x_i + \omega_{i2} \int x_i + M_i, \quad i = 1, \ldots, n, M_i > 0 \tag{16}$$

has the following conclusion: $M_i - h_i(x_i) \geq 0$; if $M_i - h_i(x_i) = 0$, there exists $x_i = 0$.

Proof: Without loss of generality, we assume that point $P(t)$ is in No. 3_i subspace, where line $P_{s1i+}P_{s2i+}$ forms the UAS h_{3i} as shown in Figture 4. Note that points P_{s1i+} and P_{s2i+} are located on the UAS h_{3i}. If we define the coordinates of points P_{s1i+}, P_{s2i+} as $P_{s1i+} = (x_1, y_1)$, $P_{s2i+} = (x_2, y_2)$, Equation (17) is obtained with the aid of Equation (6).

$$\begin{aligned} h_{3i}(P_{s1i+}) &= \omega_{3i1}x_1 + \omega_{3i2}y_1 + M_i = 0 \\ h_{3i}(P_{s2i+}) &= \omega_{3i1}x_2 + \omega_{3i2}y_2 + M_i = 0 \end{aligned} \tag{17}$$

For point $P(t)$ in Figure 4, coordinate of point $P(t)$ is given as

$$P(t) = (x_i, \int x_i) = \lambda_1 \cdot P_{s1i+} + \lambda_2 \cdot P_{s2i+} = (\lambda_1 \cdot x_1 + \lambda_2 \cdot x_2, \lambda_1 \cdot y_1 + \lambda_2 \cdot y_2) \tag{18}$$

where $\lambda_1 \geq 0$, $\lambda_2 \geq 0$. Then, with the aid of Equation (6), the conclusion (17) is obtained for point $P(t)$.

$$\begin{aligned} h_{3i}(P(t)) =& \omega_{3i1}(\lambda_1 \cdot x_1 + \lambda_2 \cdot x_2) + \omega_{3i2}(\lambda_1 \cdot y_1 + \lambda_2 \cdot y_2) + M_i \\ =& \lambda_1 \cdot (\omega_{3i1}x_1 + \omega_{3i2}y_1 + M_i) + \lambda_2 \cdot (\omega_{3i1}x_2 + \omega_{3i2}y_2 + M_i) \\ & - (\lambda_1 + \lambda_2) \cdot M_i + M_i \end{aligned} \tag{19}$$

Considering Equation (17), Equation (19) can be transformed into a simplified form.

$$M_i - h_{3i}(P(t)) = (\lambda_1 + \lambda_2) \cdot M_i \tag{20}$$

The coefficients λ_1, λ_2, M_i satisfy $\lambda_1 \geq 0$, $\lambda_2 \geq 0$ and $M_i > 0$ from previous discussion. It follows that $M_i - h_{3i}(P(t)) \geq 0$ for $P(t)$ in No. 3_i subspace. Note that there exists $\lambda_1 = 0$, $\lambda_2 = 0$ when $M_i - h_{3i}(P(t)) = 0$. Then, coordinate of $P(t)$ satisfies Equation (21) for condition $M_i - h_{3i}(P(t)) = 0$.

$$P(t) = (x_i, \int x_i) = (\lambda_1 \cdot x_1 + \lambda_2 \cdot x_2,\ \lambda_1 \cdot y_1 + \lambda_2 \cdot y_2) = (0, 0) \tag{21}$$

From the definition of current UAS $h_i(x_i)$ in Equation (8), it is clear that $h_i(x_i) = h_{3i}(x_i)$ for state x_i in No. 3_i subspace. Therefore, we have conclusion that $M_i - h_i(x_i) \geq 0$; if $M_i - h_i(x_i) = 0$, there exists $x_i = 0$ for state x_i in No. 3_i subspace. When state x_i is moving in other subspaces, we have similar conclusions. The discussion is omitted for the sake of simplicity.

Theorem 4.1. *Given system (1), assuming that approaching law N_i is a positive value, if the control law (10) is applied, system (1) is asymptotically stable.*

Proof: The Lyapunov function for system (1) is selected as

$$V = 1/2 \cdot (\boldsymbol{M} - \boldsymbol{h})^T (\boldsymbol{M} - \boldsymbol{h}) \tag{22}$$

where $\boldsymbol{h} = [h_1, \ldots, h_n]^T$, $\boldsymbol{M} = [M_1, \ldots, M_n]^T$. If we define $V_i = 1/2 \cdot (M_i - h_i)^2$, Lyapunov function V is rewritten as $V = \sum_{i=1}^{n} V_i$. From the above discussion Lemma 4.1, it is noted that function V_i is continuous. So Lyapunov function V is continuous. On the other hand, function V could deduce an obvious conclusion that $V \geq 0$; if $V = 0$, there exists $V_i = 1/2(M_i - h_i)^2 = 0$. Then, considering the discussion in Lemma 4.2, the following conclusion is obtained:

$$V \geq 0;\ \text{if } V = 0,\ \text{there exists } \boldsymbol{x} = [x_1, \cdots, x_n]^T = 0 \tag{23}$$

On the other hand, the time derivative of V along the system trajectories is expressed as:

$$\dot{V} = (\boldsymbol{M} - \boldsymbol{h})^T (\dot{\boldsymbol{M}} - \dot{\boldsymbol{h}}) \tag{24}$$

Under the definition of $\boldsymbol{M}$, $\dot{\boldsymbol{h}}$ in Step 3 and Step 4, we have the following results:

$$\begin{aligned} \dot{V} &= \sum_{i=1}^{n} \dot{V}_i \\ &= -\sum_{i=1}^{n} (M_i - h_i) \cdot N_i \end{aligned} \tag{25}$$

According to the above assumption, approaching law N_i is a positive value. Meanwhile, from Lemma 4.2, we have $M_i - h_i(x_i) \geq 0$ and if $x_i \neq 0$, there exists $M_i - h_i(x_i) > 0$. Thus, the time derivative of V_i satisfies the following conclusion:

$$\dot{V}_i \leq 0; \text{ if } \boldsymbol{x}_i \neq 0, \text{ there exists } \dot{V}_i < 0 \tag{26}$$

Considering $V = \sum_{i=1}^{n} V_i$ and $\boldsymbol{x} = [x_1, \cdots, x_n]^T$, conclusion (26) can be rewritten as

$$\dot{V} \leq 0; \text{ if } x \neq 0, \text{ there exists } \dot{V} < 0 \tag{27}$$

From conclusion (23) and (27), it is noted that system (1) is asymptotically stable.

4.2. **Positively invariant property.** In this section, we describe a set Q_i with UAS h_{ki} and provide the proof for positively invariant property in this set. As discussed in [9], the positively invariant property of Q_i is defined as follows:

Definition 4.1. [9] *The set*

$$Q_i = \{(x_i, \int x_i) | h_{ki} \geq 0, k = 0, 1, 2, 3\}, \quad i = 1, \ldots, n \tag{28}$$

is said positively invariant (PI) for a system of the form

$$\dot{\boldsymbol{x}} = \boldsymbol{f}(\boldsymbol{x}) + \boldsymbol{g}(\boldsymbol{x})\boldsymbol{u}$$

if for all $(x_i(0), \int_{-\infty}^{0} x_i(\tau)d\tau) \in Q_i$ *the solution* $(x_i(t), \int_{-\infty}^{t} x_i(\tau)d\tau) \in Q_i$ *for* $t > 0$. *If* $(x_i(0), \int_{-\infty}^{0} x_i(\tau)d\tau) \in Q_i$ *implies* $(x_i(t), \int_{-\infty}^{t} x_i(\tau)d\tau) \in Q_i$ *for all* $t > 0$ *then we say that* Q_i *is invariant.*

Theorem 4.2. *Given system (1), if the control law (10) is applied, the set* Q_i *is a positively invariant set.*

Proof: Set Q_i is proved as a PI set by using reduction to absurdity. Considering the initial state $P(0) = (x_i(0), \int_{-\infty}^{0} x_i(\tau)d\tau) \in Q_i$ in No. j_i subspaces, we assume that there exists $P(t) = (x_i(t), \int_{-\infty}^{t} x_i(\tau)d\tau) \notin Q_i$ in No. k_i subspaces, where $j, k \in \{0, 1, 2, 3\}$. From the definition of Q_i, it is noted that $h_{ji}(P(0)) \geq 0$. On the other hand, we notice that, for $P(t) \notin Q_i$ in No. k_i subspaces, there exists $h_{ki}(P(t)) < 0$ as shown in Figure 5.

From $h_{ji}(P(0)) \geq 0$ and $h_i = h_{ji}$ in No. j_i subspaces, we obtain conclusion (29).

$$V_i(P(0)) = 1/2 \cdot (M_i - h_i)^2 = 1/2 \cdot (M_i - h_{ji}(P(0)))^2 \leq 1/2 \cdot M_i^2 \tag{29}$$

From $h_{ki}(P(t)) < 0$ and $h_i = h_{ki}$ in No. k_i subspaces, we obtain conclusion (30).

$$V_i(P(t)) = 1/2 \cdot (M_i - h_i)^2 = 1/2 \cdot (M_i - h_{ki}(P(t)))^2 > 1/2 \cdot M_i^2 \tag{30}$$

Considering Equation (29) and Equation (30), there exists $V_i(P(0)) < V_i(P(t))$ for system (1). However, as discussed in Theorem 4.1, function V_i is a continuous function with negative derivative $\dot{V}_i \leq 0$. State trajectory should satisfy the conclusion $V_i(P(0)) \geq V_i(P(t))$. Then, we find the contradiction. Hence, the above assumption is incorrect. For initial state $P(0) \in Q_i$, there exists $P(t) \in Q_i$ *for all* $t > 0$. So set Q_i is a positively invariant set under Definition 4.1.

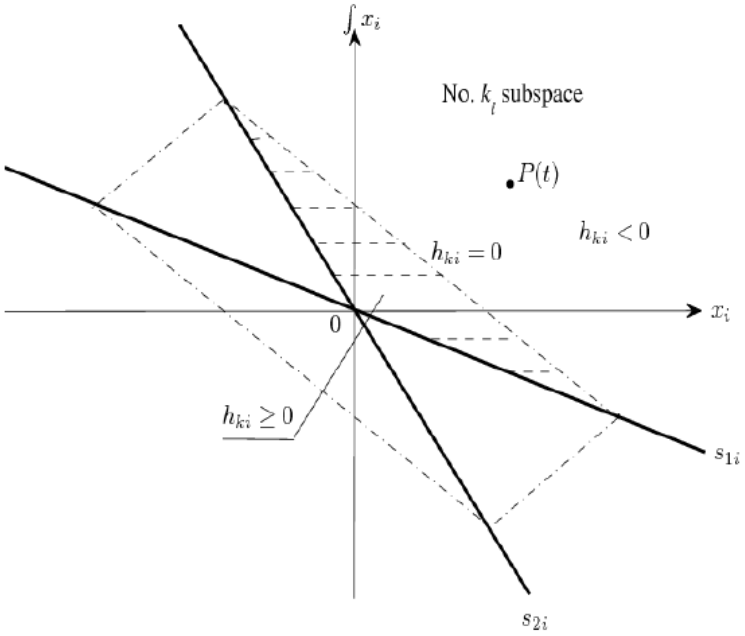

FIGURE 5. $P(t) \notin Q_i$ in No. k_i subspaces

According to Theorem 4.2, set Q_i can be proved as a positively invariant set. Then, state x_i is constrained in ψ_i for any initial state inside Q_i under the condition $Q_i \in \psi_i$. In other words, if we design set Q_i inside constraints ψ_i as shown in Figure 2, the state constraints ψ will be satisfied.

4.3. **Chattering-free design.** The above results are useful to construct a PI set with UAS-SMC method and verify if it retains invariance, but does not consider the chattering phenomenon in UAS-SMC method. This phenomenon will lead to low control accuracy and high wear of moving mechanical parts, which is harmful to the practical applications. In this section, we provide an approaching law to eliminate the chattering phenomenon in UAS-SMC method. This chattering-free approaching law N_i is defined as:

$$N_i = \omega_{i2} \cdot x_i + \omega_{i1}\{\kappa_i(a_i \cdot x_i - k_i \cdot s_{2i}) + (1 - \kappa_i)[1/2 \cdot (a_i + b_i)x_i]\} \tag{31}$$

where $k_i > 0$, $a_i = -\omega_{0i2}/\omega_{0i1} = -\omega_{3i2}/\omega_{3i1}$, $b_i = -\omega_{1i2}/\omega_{1i1} = -\omega_{2i2}/\omega_{2i1}$

$$\kappa_i = \begin{cases} |s_{2i}|/(|s_{1i}| + |s_{2i}|) & s_{1i} \cdot s_{2i} \leq 0, s_{1i} \neq 0 \\ |s_{2i}|/(|s_{2i}| + |x_i|) & s_{2i}x_i \leq 0, x_i \neq 0 \\ 1 & s_{1i}x_i \geq 0 \end{cases}$$

In the following, two lemmas are given to prove the chattering-free property in approaching law (31):

Lemma 4.3. *If the switching surfaces s_{1i}, s_{2i} satisfy $\xi_{1i} > \xi_{2i} > 0$ and points P_{s1i+}, P_{s2i-}, P_{s1i-}, P_{s2i-} are selected as shown in Step 2, there exist $\omega_{0i1} > 0$, $\omega_{0i2} > 0$, $\omega_{3i1} < 0$, $\omega_{3i2} < 0$.*

Proof: As shown in Figure 6, line $P_{s1i-}P_{s2i-}$ is called UAS h_{0i} in No. 0_i subspace, where points P_{s1i-} and P_{s2i-} are located in the fourth and the second quadrants respectively. It follows that h_{0i} passes through the third quadrant. Then, there exist points $C = (0, c)$ and $D = (d, 0)$, $c < 0$, $d < 0$ on the UAS h_{0i}. Considering Equation (6), we obtain the

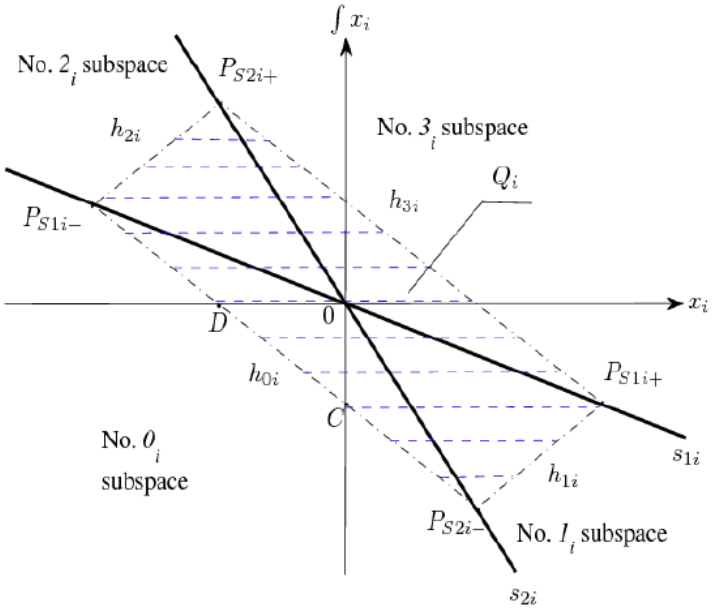

FIGURE 6. The location of UAS h_{0i}

following equations

$$\begin{aligned} h_{0i}(C) &= \omega_{0i1} \cdot 0 + \omega_{0i2} \cdot c + M_i = 0 \\ h_{0i}(D) &= \omega_{0i1} \cdot d + \omega_{0i2} \cdot 0 + M_i = 0 \end{aligned} \tag{32}$$

where $M_i > 0$, coefficients ω_{0i1} and ω_{0i2} can be expressed as

$$\omega_{0i1} = -M_i/d; \quad \omega_{0i2} = -M_i/c \tag{33}$$

Note that there exist $c < 0$, $d < 0$ and $M_i > 0$, we have conclusion $\omega_{0i1} > 0$, $\omega_{0i2} > 0$. Similarly, the conclusion $\omega_{3i1} < 0$, $\omega_{3i2} < 0$ is obtained.

Lemma 4.4. *If the coefficients ω_{1i1}, ω_{1i2} in Equation (6) satisfy the chattering-free condition $\omega_{1i1} < 0$, $\omega_{2i1} > 0$, we have inequality $a_i < b_i$, where the coefficients are expressed as*

$$a_i = -\omega_{0i2}/\omega_{0i1} = -\omega_{3i2}/\omega_{3i1}, \quad b_i = -\omega_{1i2}/\omega_{1i1} = -\omega_{2i2}/\omega_{2i1}$$

Proof: According to Equation (6), UAS h_{1i} is given as follows:

$$h_{1i} = \omega_{1i1} x_i + \omega_{1i2} \int x_i + M_i \tag{34}$$

Note that UAS h_{1i} can be located in three different areas, namely, Area 1, Beyond 2 and Beyond 3 in Figure 7, where the definitions of these areas are given as:

Area 1 $= \{h_{1i} | b_i = -\omega_{1i2}/\omega_{1i1} < -\xi_{2i}^{-1}, h_{1i}(P_{s2i-}) = 0\}$; Beyond 2 $= \{h_{1i} | 0 > b_i = -\omega_{1i2}/\omega_{1i1} > -\xi_{2i}^{-1}, h_{1i}(P_{s2i-}) = 0\}$; Beyond 3 $= \{h_{1i} | b_i = -\omega_{1i2}/\omega_{1i1} > 0, h_{1i}(P_{s2i-}) = 0\}$.

For surface h_{1i} in Beyond 2, the discussion is shown as follows:

As shown in Figure 8, there exists a point $E = (e, 0)$, $e < 0$ on the surface h_{1i}. If we substitute $E = (e, 0)$ into Equation (34), condition $\omega_{1i1} = -M_i/e > 0$ will be obtained. However, coefficient ω_{1i1} should satisfy the chattering-free condition $\omega_{1i1} < 0$. So UAS h_{1i} in Beyond 2 is not considered in this paper.

For the surface h_{1i} in Beyond 3, the discussion is given as:

As shown in Figure 9, there exists a point $F = (0, f)$, $f < 0$ on the surface h_{1i}. If we substitute $F = (0, f)$ into Equation (34), condition $\omega_{1i2} = -M_i/f \geq 0$ is obtained. Note the coefficient ω_{1i1} should satisfy the chattering-free condition $\omega_{1i1} < 0$. Then, we have

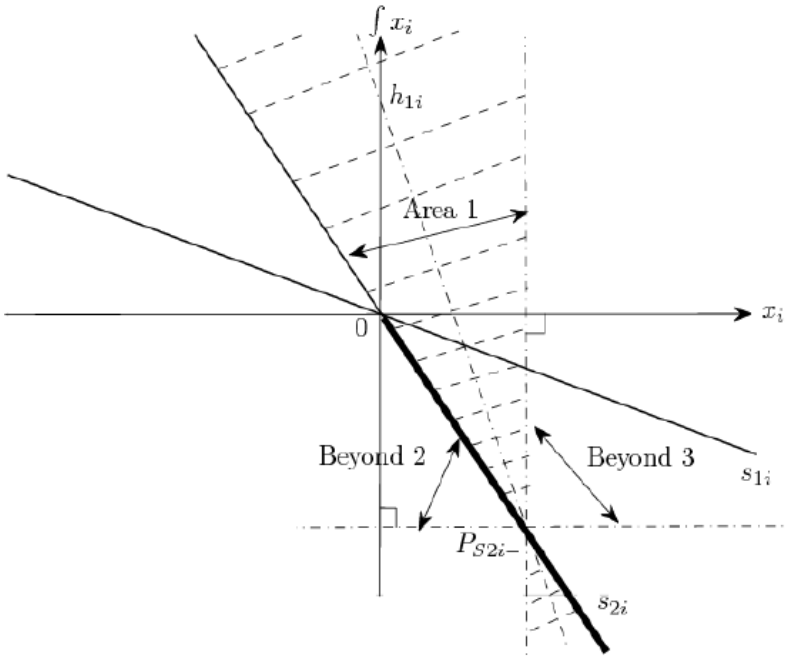

FIGURE 7. UAS h_{1i} in Area 1, Beyond 2 and Beyond 3

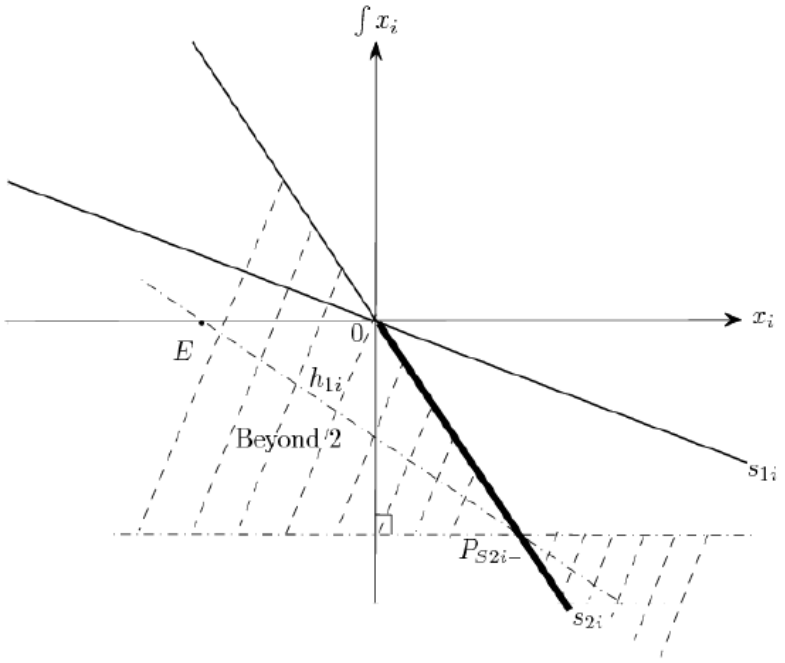

FIGURE 8. UAS h_{1i} in Beyond 2

result $b_i = -\omega_{1i2}/\omega_{1i1} \geq 0$. On the other hand, there exists result $a_i = -\omega_{0i2}/\omega_{0i1} < 0$ as shown in Lemma 4.3. Thus, conclusion $a_i < b_i$ is obtained.

For the surface h_{1i} in Area 1, the discussion is given as:

According to the expression in Equation (6), the formula of $h_{0i} = 0$ and $h_{1i} = 0$ can be transformed into the following form.

$$\int x_i = -\omega_{0i1}/\omega_{0i2} \cdot xi - M_i/\omega_{0i2}; \quad \int x_i = -\omega_{1i1}/\omega_{1i2} \cdot xi - M_i/\omega_{1i2} \tag{35}$$

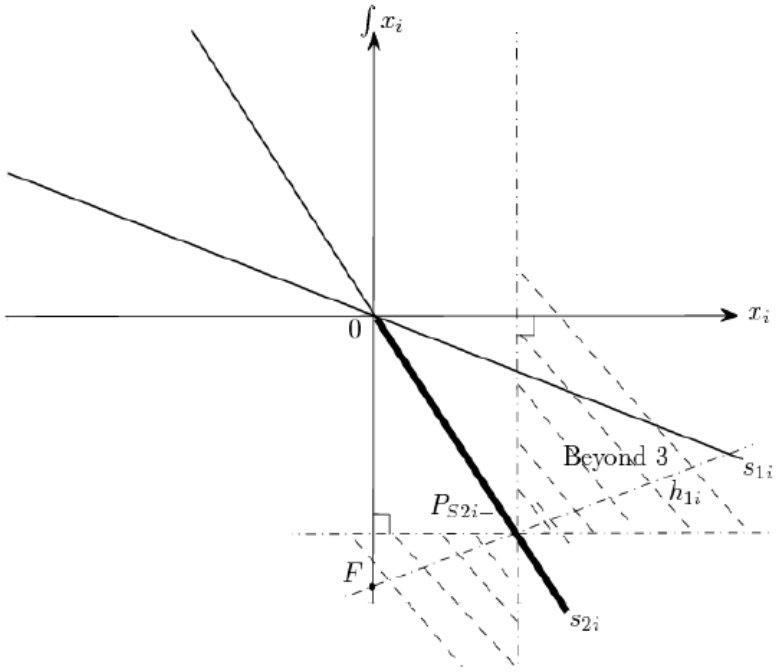

FIGURE 9. UAS h_{1i} in Beyond 3

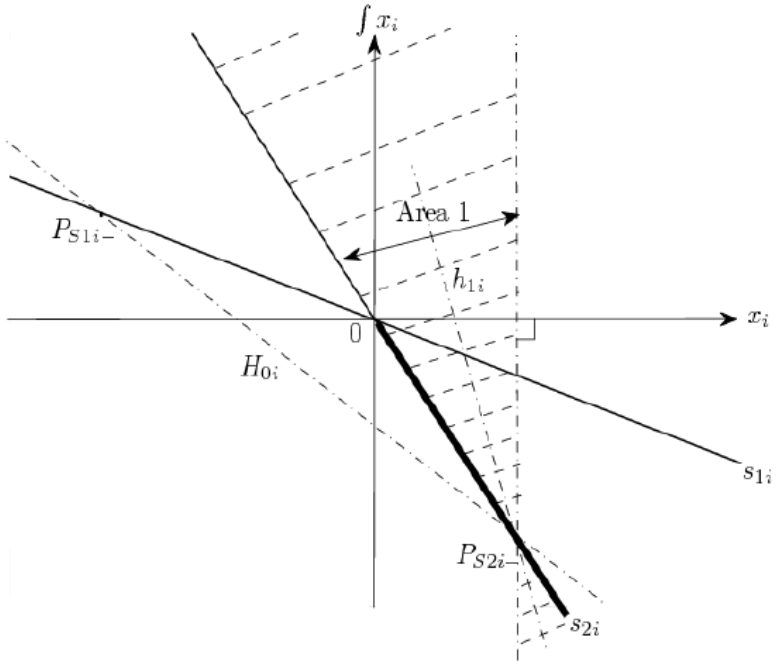

FIGURE 10. UAS h_{1i} in Area 1

Note that coefficients ω_{0i1}, ω_{0i2} need to satisfy $\omega_{0i1} > 0$, $\omega_{0i2} > 0$ in Lemma 4.3. Then, the gradients of $h_{0i} = 0$ and $h_{1i} = 0$ are given as $-\omega_{0i1}/\omega_{0i2} < 0$ and $-\omega_{1i1}/\omega_{1i2}$ respectively.

Considering the gradient of $h_{0i} = 0$ in Figure 10, the gradient of $h_{1i} = 0$ in Area 1 is more attached to negative infinity. So we obtain result (36)

$$-\omega_{1i1}/\omega_{1i2} < -\omega_{0i1}/\omega_{0i2} < 0 \tag{36}$$

Taking the reciprocals of elements in Equation (36), it is noted that

$$0 > -\omega_{1i2}/\omega_{1i1} > -\omega_{0i2}/\omega_{0i1} \tag{37}$$

According to the definitions of a_i, b_i in Equation (31), we have $a_i = -\omega_{0i2}/\omega_{0i1} = -\omega_{3i2}/\omega_{3i1}$, $b_i = -\omega_{1i2}/\omega_{1i1} = -\omega_{2i2}/\omega_{2i1}$. Then, $a_i < b_i$ is obtained. Considering the above results, it is clear that, if the coefficients ω_{1i1}, ω_{1i2} satisfy $\omega_{1i1} < 0$, $\omega_{2i1} > 0$, there exists $a_i < b_i$.

Theorem 4.3. *Given system (1), if chattering-free condition $\omega_{1i1} < 0$, $\omega_{2i1} > 0$ and simplified condition (7) are satisfied, the system with UAS-SMC controller (10) and approaching law (31) is chattering-free and stable.*

Proof: First of all, a discussion is required for the demonstration. The purpose of this theorem is to design a chattering-free UAS-SMC controller (10). As the chattering-free approaching law is predefined in Equation (31), what we need to do is to verify the continuous and stable property. Then, proof in this theorem falls into two different parts. The first part relates to the chattering-free property. And the second part focuses on the stability of UAS-SMC controller.

(1) Chattering-free Property

Note that the formula κ_i in Equation (31) is written as:

$$\kappa_i = \begin{cases} |s_{2i}|/(|s_{1i}| + |s_{2i}|) & s_{1i} \cdot s_{2i} \le 0, s_{1i} \neq 0 \\ |s_{2i}|/(|s_{2i}| + |x_i|) & s_{2i} x_i \le 0, x_i \neq 0 \\ 1 & s_{1i} x_i \ge 0 \end{cases} \tag{38}$$

Considering Equation (38), we can obtain the following conclusions:

When $s_{1i} = 0$, $|s_{2i}|/(|s_{1i}|+|s_{2i}|) = 1$; when $s_{2i} = 0$, $|s_{2i}|/(|s_{2i}|+|x_i|) = 0$ and $|s_{2i}|/(|s_{1i}|+|s_{2i}|) = 0$; when $x_i = 0$, $|s_{2i}|/(|s_{2i}| + |x_i|) = 1$. Thus, κ_i in Equation (38) is continuous.

According to the design process in Step 3, coefficients $\boldsymbol{\Omega}_1$, $\boldsymbol{\Omega}_2$ and $\boldsymbol{N}$ are predefined as

$$\boldsymbol{\Omega}_1 = \text{diag}\{\omega_{11}, \ldots, \omega_{n1}\}, \quad \boldsymbol{\Omega}_2 = \text{diag}\{\omega_{12}, \ldots, \omega_{n2}\}, \quad \boldsymbol{N} = [N_1, \ldots, N_n]^T$$

Then, the elements in $-\boldsymbol{\Omega}_1^{-1}\boldsymbol{\Omega}_2 \cdot \boldsymbol{x} + \boldsymbol{\Omega}_1^{-1} \cdot \boldsymbol{N}$ can be expressed as follows:

$$-\boldsymbol{\Omega}_1^{-1}\boldsymbol{\Omega}_2 \cdot \boldsymbol{x} + \boldsymbol{\Omega}_1^{-1} \cdot \boldsymbol{N} = [-\omega_{11}^{-1}\omega_{12} \cdot x_1 + \omega_{11}^{-1}N_1, \ldots, -\omega_{n1}^{-1}\omega_{n2} \cdot x_n + \omega_{n1}^{-1}N_n]^T \tag{39}$$

If we define function φ_i as

$$\varphi_i = -\omega_{i1}^{-1}\omega_{i2} \cdot x_i + \omega_{i1}^{-1}N_i, \quad i = 1, \ldots, n \tag{40}$$

conclusion (41) is obtained by substituting Equation (31) into Equation (40).

$$\varphi_i = \kappa_i(a_i \cdot x_i - k_i \cdot s_{2i}) + (1 - \kappa_i)[1/2 \cdot (a_i + b_i)x_i] \tag{41}$$

Note that elements κ_i, $(a_i \cdot x_i - k_i \cdot s_{2i})$ and $[1/2 \cdot (a_i + b_i)x_i]$ are continuous, the element φ_i in $\boldsymbol{\Omega}_1^{-1}\boldsymbol{\Omega}_2 \cdot \boldsymbol{x} + \boldsymbol{\Omega}_1^{-1} \cdot \boldsymbol{N}$ is a continuous function. Considering the continuity of $\boldsymbol{f}(\boldsymbol{x})$, $\boldsymbol{g}(\boldsymbol{x})$ and $\boldsymbol{\Omega}_1^{-1}\boldsymbol{\Omega}_2 \cdot \boldsymbol{x} + \boldsymbol{\Omega}_1^{-1} \cdot \boldsymbol{N}$, UAS-SMC controller (10) with approaching law (31) is continuous. Then, the system is chattering-free.

(2) Stable Property

The stable property of UAS-SMC controller with chattering-free approaching law (31) is given in this part. Firstly, we will prove that approaching law (31) satisfies $N_i \ge 0$ and $N_i = 0$ if and only if $x_i = 0$, $\int x_i = 0$.

As shown in Figure 11, the state space is divided into three subspaces: $s_{1i} \cdot s_{2i} \le 0$; $s_{2i} \cdot x_i \le 0$; $s_{1i} \cdot x_i \ge 0$. Then, for state x_i in subspace $s_{1i} \cdot s_{2i} \le 0$, the discussion is given as follows:

When state x_i satisfies $s_{1i} \ge 0$, $s_{2i} \le 0$, it is noted that the point $(x_i, \int x_i)$ is located in No. 2_i subspace by comparing Figure 1 and Figure 11. Then, we have $\omega_{i1} = \omega_{2i1} > 0$, $\omega_{i2} = \omega_{2i2}$, $x_i \le 0$, $s_{2i} \le 0$, $k_i > 0$ and $b_i = -\omega_{2i2}/\omega_{2i1}$ from the definitions in Step 3 and Step 4. According to Lemma 4.4, conclusion $a_i < b_i$ is obtained. So there exist $a_i \cdot x_i - k_i \cdot s_{2i} \ge b_i \cdot x_i$ and $1/2 \cdot (a_i + b_i)x_i \ge b_i \cdot x_i$. On the other hand, $0 \le \kappa_i \le 1$

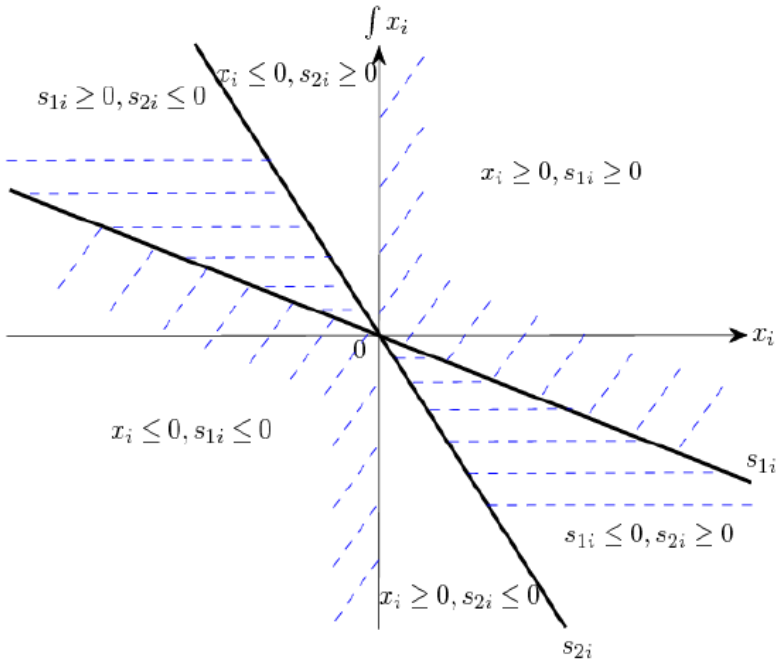

FIGURE 11. The subspaces in the state space

is obtained from the formula form of κ_i in Equation (38). With above conclusions, it is clear that

$$\kappa_i(a_i \cdot x_i - k_i \cdot s_{2i}) + (1-\kappa_i)[1/2 \cdot (a_i + b_i)x_i] \ge b_i \cdot x_i.$$

If we substitute this inequality into the approaching law (31), the following result is obtained:

$$N_i = \omega_{i2} \cdot x_i + \omega_{i1}\{\kappa_i(a_i \cdot x_i - k_i \cdot s_{2i}) + (1-\kappa_i)[1/2 \cdot (a_i + b_i)x_i]\} \ge \omega_{2i2} \cdot x_i + \omega_{2i1} \cdot b_i \cdot x_i = 0 \quad (42)$$

where $N_i = 0$ if and only if $x_i = 0$, $\int x_i = 0$.

Similarly, for state x_i satisfies $s_{1i} \le 0$, $s_{2i} \ge 0$, there exist

$$N_i = \omega_{i2} \cdot x_i + \omega_{i1}\{\kappa_i(a_i \cdot x_i - k_i \cdot s_{2i}) + (1-\kappa_i)[1/2 \cdot (a_i + b_i)x_i]\} \ge \omega_{1i2} \cdot x_i + \omega_{1i1} \cdot b_i \cdot x_i = 0 \quad (43)$$

where $N_i = 0$ if and only if $x_i = 0$, $\int x_i = 0$.

For state x_i in subspaces $s_{2i} \cdot x_i \le 0$ and $s_{1i} \cdot x_i \ge 0$, we can also infer that $N_i \ge 0$, where $N_i = 0$ if and only if $x_i = 0$, $\int x_i = 0$. For the sake of simplicity, the detail discussion is omitted here.

According to above discussion, chattering-free approaching law satisfies that $N_i \ge 0$ and $N_i = 0$ if and only if $x_i = 0$, $\int x_i = 0$. Then, there exists $N_i > 0$ for $x_i \ne 0$. Considering Theorem 4.1, the stability of system is guaranteed. Note that the chattering-free property of UAS-SMC controller with approaching law (31) is already proved in the previous discussion. Then, the proof for Theorem 4.3 is finished.

5. **Simulation Experiment.** In this section, a discussion is given to show the difference between conventional SMC and chattering UAS-SMC methods.

Considering the following nonlinear system:

$$\dot{\boldsymbol{x}} = \boldsymbol{f}(\boldsymbol{x}) + \boldsymbol{g}(\boldsymbol{x})\boldsymbol{u} \quad (44)$$

where $\boldsymbol{x} = [x_1, x_2]^T$, $\boldsymbol{f}(\boldsymbol{x}) = [-2x_1 + 2x_1x_2 + 2 \cdot \sin(x_2), -x_2 \cdot \cos(x_1)]^T$, $\boldsymbol{g}(\boldsymbol{x}) = \mathrm{diag}\{1, 1\}$, $\boldsymbol{u} = [u_1, u_2]^T$.

It is assumed that the initial states are $x_1(0) = 0.275$, $\int_{-\infty}^{0} x_1(t)dt = -0.55$; $x_2(0) = -0.275$, $\int_{-\infty}^{0} x_2(t)dt = -0.55$. And the state constraints for system (44) are given as:

$$\psi = \left\{ \boldsymbol{x} | \boldsymbol{x} = [x_1, x_2]^T, -0.55 \leq x_i \leq 0.55, i = 1, 2 \right\} \tag{45}$$

According to the design process in Section 3, chattering-free UAS-SMC controller can be designed as follows:

Step 1: The switching surfaces are given as follows:

$$\begin{aligned} \boldsymbol{s}_1 &= \boldsymbol{x} + \boldsymbol{\xi}_1 \int \boldsymbol{x} = 0 \\ \boldsymbol{s}_2 &= \boldsymbol{x} + \boldsymbol{\xi}_2 \int \boldsymbol{x} = 0 \end{aligned} \tag{46}$$

where $\boldsymbol{s}_1 = [s_{11}, s_{12}]^T$, $\boldsymbol{s}_2 = [s_{21}, s_{22}]^T$, $\int \boldsymbol{x} = [\int x_1, \int x_2]^T$, $\boldsymbol{\xi}_1 = \text{diag}\{2, 2\}, \boldsymbol{\xi}_2 = \text{diag}\{0.5, 0.5\}$.

Step 2: Considering the state constraints $-0.55 \leq x_i \leq 0.55$, points P_{s1i+}, P_{s1i-}, P_{s2i+}, P_{s2i-} are selected as shown in Figure 12, where $P_{s1i+} = (0.55, -0.275)$, $P_{s1i-} = (-0.55, 0.275)$, $P_{s2i+} = (-0.275, 0.55)$, $P_{s2i-} = (0.275, -0.55)$.

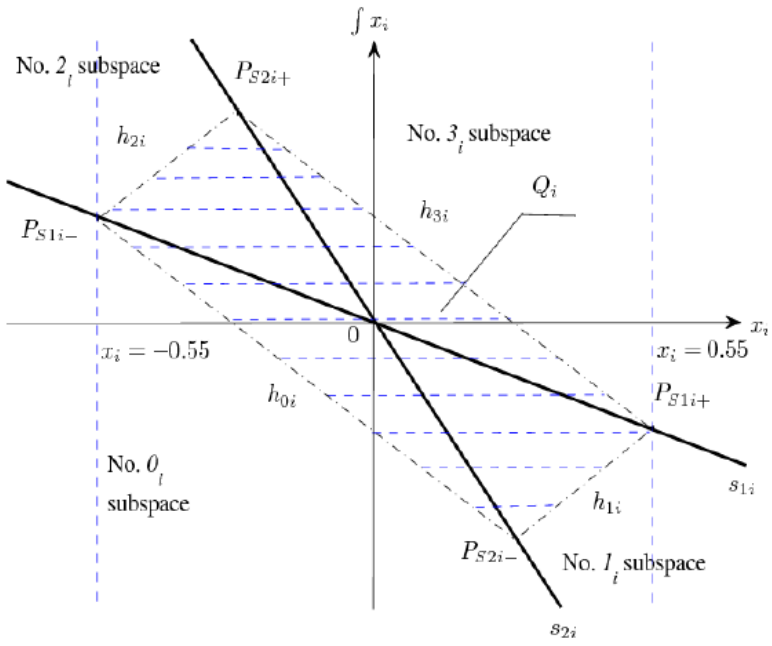

FIGURE 12. The UAS h_{0i}, h_{1i}, h_{2i}, h_{3i}

Coordinates of points P_{s1i+}, P_{s1i-}, P_{s2i+}, P_{s2i-} can be used to design UAS h_{0i}, h_{1i}, h_{2i}, h_{3i}. Then, the formulae of h_{0i}, h_{1i}, h_{2i}, h_{3i} are given as follows:

$$\begin{aligned} h_{0i} &= 1/0.275 \cdot x_i + 1/0.275 \cdot \int x_i + 1 \\ h_{1i} &= -1/0.825 \cdot x_i + 1/0.825 \cdot \int x_i + 1 \\ h_{2i} &= 1/0.825 \cdot x_i - 1/0.825 \cdot \int x_i + 1 \\ h_{3i} &= -1/0.275 \cdot x_i - 1/0.275 \cdot \int x_i + 1 \end{aligned} \tag{47}$$

Step 3: According to the UAS in Figure 12 input $\boldsymbol{u}$, current UAS h_i can be expressed as:

$$h_i = \omega_{i1} x_i + \omega_{i2} \int x_i + M_i, \quad i = 1, 2 \tag{48}$$

where

$$\omega_{i1} = \begin{cases} 1/0.275 & s_{1i} < 0, s_{2i} < 0 \\ -1/0.825 & s_{1i} < 0, s_{2i} \geq 0 \\ 1/0.825 & s_{1i} \geq 0, s_{2i} < 0 \\ -1/0.275 & s_{1i} \geq 0, s_{2i} \geq 0 \end{cases}, \quad \omega_{i2} = \begin{cases} 1/0.275 & s_{1i} < 0, s_{2i} < 0 \\ 1/0.825 & s_{1i} < 0, s_{2i} \geq 0 \\ -1/0.825 & s_{1i} \geq 0, s_{2i} < 0 \\ -1/0.275 & s_{1i} \geq 0, s_{2i} \geq 0 \end{cases}, \quad M_i = 1$$

Consequently, the compact form of current UAS is rewritten as:

$$\boldsymbol{h} = \boldsymbol{\Omega}_1 \boldsymbol{x} + \boldsymbol{\Omega}_2 \int \boldsymbol{x} + \boldsymbol{M} \tag{49}$$

where $\boldsymbol{h} = [h_1, h_2]^T$, $\boldsymbol{\Omega}_1 = \text{diag}\{\omega_{11}, \omega_{21}\}$, $\boldsymbol{\Omega}_2 = \text{diag}\{\omega_{12}, \omega_{22}\}$, $\boldsymbol{M} = [M_1, M_2]^T$.

Step 4: The chattering-free UAS-SMC controller for system (44) is expressed as:

$$\boldsymbol{u} = \boldsymbol{g}(\boldsymbol{x})^{-1}(-\boldsymbol{f}(\boldsymbol{x}) - \boldsymbol{\Omega}_1^{-1}\boldsymbol{\Omega}_2 \cdot \boldsymbol{x} + \boldsymbol{\Omega}_1^{-1} \cdot \boldsymbol{N}) \tag{50}$$

where $\boldsymbol{N} = [N_1, N_2]^T$. From the discussion in Section 4.3, the chattering-free approaching law N_i is expressed as

$$N_i = \omega_{i2} \cdot x_i + \omega_{i1}\{\kappa_i(a_i \cdot x_i - k_i \cdot s_{2i}) + (1 - \kappa_i)[1/2 \cdot (a_i + b_i)x_i]\} \tag{51}$$

where $a_i = -1$, $b_i = 1$, $k_i = 10$

$$\kappa_i = \begin{cases} |s_{2i}| / (|s_{1i}| + |s_{2i}|) & s_{1i} \cdot s_{2i} \leq 0 \\ |s_{2i}| / (|s_{2i}| + |x_i|) & s_{2i} x_i \leq 0 \\ 1 & s_{1i} x_i \geq 0 \end{cases}$$

The simulation results of state x_1, x_2 with chattering-free UAS-SMC and conventional SMC methods are given as follows.

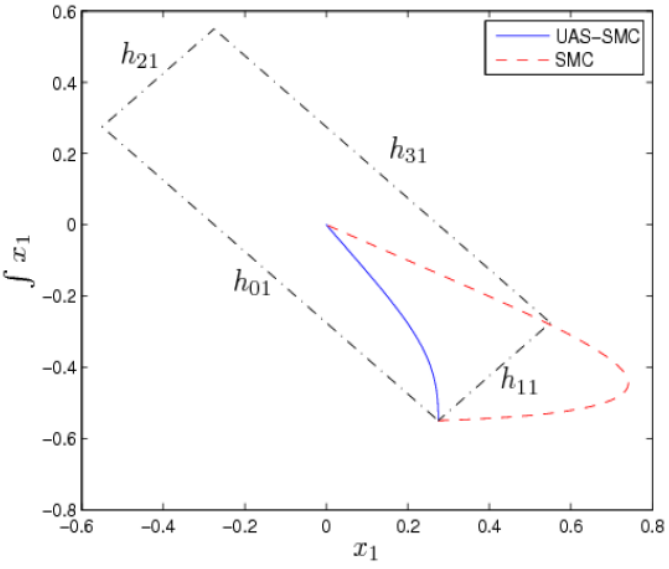

FIGURE 13. Trajectory of point $(x_1, \int x_1)$

Figure 13 and Figure 14 show the trajectories of state $\boldsymbol{x}$ with chattering-free UAS-SMC and conventional SMC strategies. Note that state x_i $(i = 1, 2)$ is constrained in state constraint ψ under chattering-free UAS-SMC method. However, the constraint is not satisfied under SMC controller as shown in Figure 13 and Figure 14. Figure 15 shows the control inputs u_1 and u_2 with chattering-free approaching law N_i. It is clear that chattering phenomenon is eliminated with chattering-free approaching law (31).

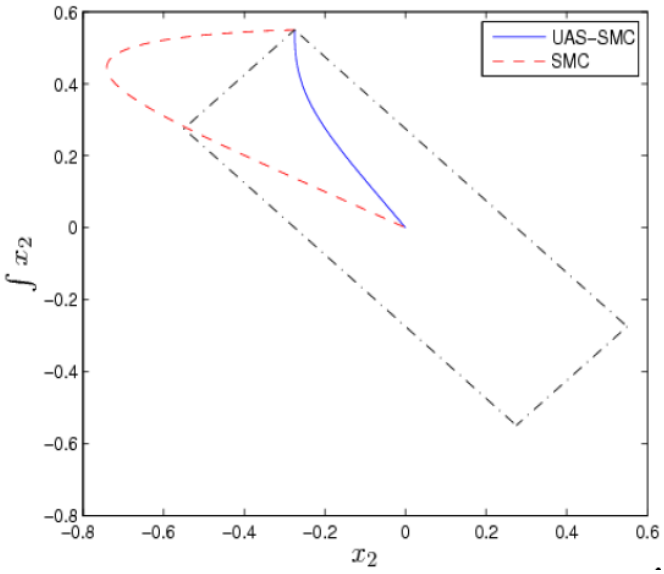

FIGURE 14. Trajectory of point $(x_2, \int x_2)$

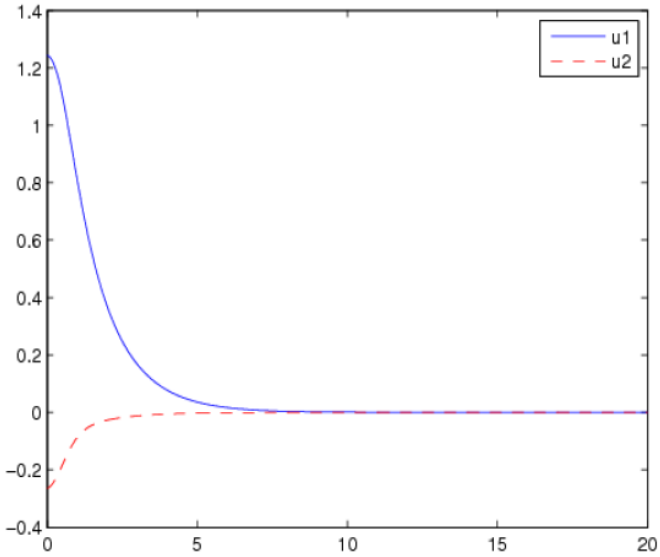

FIGURE 15. Control inputs of chattering-free UAS-SMC

6. **Conclusions.** An innovative method called sliding mode control with unidirectional auxiliary surfaces (UAS-SMC) is proposed in this paper. The main advantage of this design is that system states are constrained by unidirectional auxiliary surfaces instead of switching surfaces. Then, constraints are guaranteed when system states leaving the switching surfaces. On the other hand, a chattering-free approaching law is given to eliminate the chattering phenomenon in the controller. As shown in the examples, the proposed strategy can guarantee the satisfaction of state constraints and avoid the overshoots in the system.

Acknowledgment. This work is partially supported by the National Natural Science Foundation of China [grant numbers 91116017, 60974106, 61174102]; Priority Academic Program Development of Jiangsu Higher Education Institution. The authors also gratefully acknowledge the helpful comments and suggestions of the reviewers, which have improved the presentation.

REFERENCES

[1] L. Wu, X. Su and P. Shi, Sliding mode control with bounded L_2 gain performance of Markovian jump singular time-delay systems, *Automatica*, vol.48, no.8, pp.1929-1933, 2012.

[2] Z. Gao, B. Jiang, P. Shi, M. Qian and J. Lin, Active fault tolerant control design for reusable launch vehicle using adaptive sliding mode approach, *J. of Franklin Institute*, vol.349, no.4, pp.1543-1560, 2012.

[3] M. Liu, P. Shi, L. Zhang and X. Zhao, Fault tolerant control for nonlinear Markovian jump systems via proportional and derivative sliding mode observer, *IEEE Trans. on Circuits and Systems I: Regular Papers*, vol.58, no.11, pp.2755-2764, 2011.

[4] L. Wu, P. Shi and H. Gao, State estimation and sliding mode control of Markovian jump singular systems, *IEEE Trans. on Automatic Control*, vol.55, no.5, pp.1213-1219, 2010.

[5] J. Zhang, P. Shi and Y. Xia, Robust adaptive sliding mode control for fuzzy systems with mismatched uncertainties, *IEEE Trans. on Fuzzy Systems*, vol.18, no.4, pp.700-711, 2010.

[6] M. Rubagotti and A. Ferrara, Second order sliding mode control of a perturbed double integrator with state constraints, *American Control Conference Marriott Waterfront*, Baltimore, MD, USA, 2010.

[7] H. Tanizawa and Y. Ohta, Sliding mode control under state and control constraints, *The 16th IEEE International Conference on Control Applications Part of IEEE Multi-Conference on Systems and Control Singapore*, 2007.

[8] A. Bartoszewicz and A. Nowacka, An optimal switching plane design for the third order system subject to state constraints, *Proc. of the 2006 International Workshop on Variable Structure Systems*, Alghero, Italy, 2006.

[9] F. Blanchini, Set invariance in control, *Automatica*, vol.35, no.11, pp.1747-1767, 1999.

[10] B. D. O'Dell and E. A. Misawa, Semi-ellipsoidal controlled invariant sets for constrained linear systems, *ASME Journal on Dynamic Systems, Measurements and Control*, vol.124, pp.98-103, 2002.

[11] H. Richter, Constrained sliding mode control: Invariant cylinder methodology, variable structure systems, *VSS'08 International Workshop*, 2008.

[12] J. Fu, Q. Wu, W. Chen and X. Yan, Chattering-free condition for sliding mode control with unidirectional auxiliary surfaces, *Transactions of the Institute of Measurement and Control*, 2012.